

Free quarks and antiquarks versus hadronic matter^{*}

XU Xiao-Ming(许晓明)^{1,1)} PENG Ru(彭茹)²⁾

1 (Department of Physics, Shanghai University, Baoshan, Shanghai 200444, China)

2 (Department of Physics, Wuhan University of Science and Technology, Wuhan 430081, China)

Abstract Meson-meson reactions $A(q_1 \bar{q}_1) + B(q_2 \bar{q}_2) \rightarrow q_1 + \bar{q}_1 + q_2 + \bar{q}_2$ in high-temperature hadronic matter are found to produce an appreciable amount of quarks and antiquarks freely moving in hadronic matter and to establish a new mechanism for deconfinement of quarks and antiquarks in hadronic matter.

Key words free quarks, hadronic matter, deconfinement

PACS 25.75.-q, 25.75.Nq, 12.38.Mh

1 Introduction

The picture for hadronic matter is that this matter only consists of hadrons and the evolution of this matter is determined by hadron scatterings and hadron flows. Meson-meson elastic scatterings establish thermal states of hadronic matter. At the critical temperature T_c of QCD phase transition quarks and antiquarks automatically move from the small hadron volume toward the large volume of hadronic matter. However, in the present work we show that this pure hadronic matter below T_c is mixed with free quarks and antiquarks. The reason is that meson-meson scatterings into free quarks and free antiquarks $A(q_1 \bar{q}_1) + B(q_2 \bar{q}_2) \rightarrow q_1 + \bar{q}_1 + q_2 + \bar{q}_2$ at high temperature can cause the ratio of free quark number density to hadronic matter number density to be larger than 0.05 in a small time period of 1 fm/c. There-

fore, the reactions offer a new way for deconfinement near the critical temperature, and we name such a type of deconfinement collisional deconfinement. We address the occurrence of deconfinement from variation of number densities of hadrons and free quarks and antiquarks in contrast to the variation of energy density, chiral condensate and the screening mass of a heavy quark-antiquark pair studied by lattice QCD^[1]. We focus on the reactions of π , ρ , K and K^* because they are dominant meson species in hadronic matter at RHIC^[2-4].

2 Cross sections and master rate equations

The cross section for $A(q_1 \bar{q}_1) + B(q_2 \bar{q}_2) \rightarrow q_1 + \bar{q}_1 + q_2 + \bar{q}_2$ is

$$\begin{aligned} \sigma = & \frac{(2\pi)^4}{4\sqrt{(P_A \cdot P_B)^2 - m_A^2 m_B^2}} \int \frac{d^3 p_{q'_1}}{(2\pi)^3 2E_{q'_1}} \frac{d^3 p_{\bar{q}'_1}}{(2\pi)^3 2E_{\bar{q}'_1}} \frac{d^3 p_{q'_2}}{(2\pi)^3 2E_{q'_2}} \frac{d^3 p_{\bar{q}'_2}}{(2\pi)^3 2E_{\bar{q}'_2}} \times \\ & |\mathcal{M}_{\bar{q}}|^2 \delta(P_A + P_B - p_{q'_1} - p_{\bar{q}'_1} - p_{q'_2} - p_{\bar{q}'_2}) = \\ & \frac{1}{32(2\pi)^8 \sqrt{[s - (m_A + m_B)^2][s - (m_A - m_B)^2]}} \int d\Omega_{q'_2} \frac{d^3 p_{q'_1}}{E_{q'_1}} \frac{d^3 p_{\bar{q}'_1}}{E_{\bar{q}'_1}} \times \\ & \frac{\mathbf{p}_{q'_2}^2 |\mathcal{M}_{\bar{q}}|^2}{|\mathbf{p}_{q'_2} | E_{q'_2} + (|\mathbf{p}_{q'_2} | - |\mathbf{P}_A + \mathbf{P}_B - \mathbf{p}_{q'_1} - \mathbf{p}_{\bar{q}'_1} | \cos \Theta) E_{q'_2}} | \end{aligned} \quad (1)$$

Received 2 December 2008

^{*} Supported by National Natural Science Foundation of China (10675079)

1) E-mail: xmxu@mail.shu.edu.cn

©2009 Chinese Physical Society and the Institute of High Energy Physics of the Chinese Academy of Sciences and the Institute of Modern Physics of the Chinese Academy of Sciences and IOP Publishing Ltd

where $s = (P_A + P_B)^2$ with the mass m_A (m_B) and the four-momentum P_A (P_B) of meson A(B); $p_i = (E_i, \mathbf{p}_i)$ ($i = q'_1, \bar{q}'_1, q'_2, \bar{q}'_2$) is the four-momentum of a final quark or antiquark, and subscripts of variables for the final quarks and antiquarks are labeled with primes; Θ is the angle between $\mathbf{p}_{q'_2}$ and $\mathbf{P}_A + \mathbf{P}_B - \mathbf{p}_{q'_1} - \mathbf{p}_{\bar{q}'_1}$, and $d\Omega_{q'_2}$ is the solid angle centered about the direction of $\mathbf{p}_{q'_2}$. At present, we consider only the diagrams in Fig. 1 coming from one gluon exchange between one constituent in meson A and one constituent in meson B.

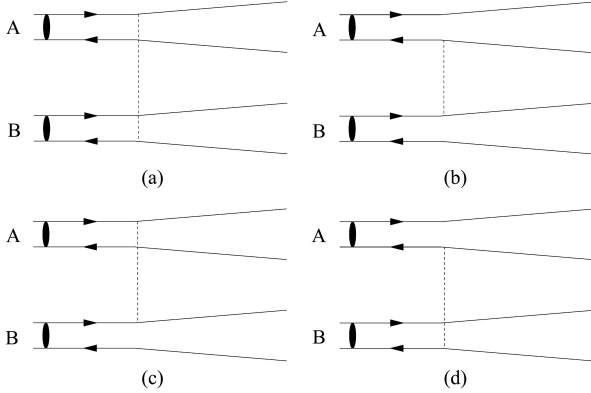


Fig. 1. Diagrams for $A(q_1 \bar{q}_1) + B(q_2 \bar{q}_2) \rightarrow q_1 + \bar{q}_1 + q_2 + \bar{q}_2$.

The corresponding transition amplitude \mathcal{M}_{fi} is

$$\begin{aligned} \mathcal{M}_{\text{fi}} = & \sqrt{2E_A 2E_B 2E_{q'_1} 2E_{\bar{q}'_1} 2E_{q'_2} 2E_{\bar{q}'_2}} \times \\ & \left[\psi_{cs}^+ V_{q_1 \bar{q}_2}(\mathbf{Q}) \psi_{q_1 \bar{q}_1} \left(\mathbf{p}_{q'_1 \bar{q}'_1} - \frac{m_{\bar{q}_1}}{m_{q_1} + m_{\bar{q}_1}} \mathbf{Q} \right) \times \right. \\ & \psi_{q_2 \bar{q}_2} \left(\mathbf{p}_{q'_2 \bar{q}'_2} - \frac{m_{q_2}}{m_{q_2} + m_{\bar{q}_2}} \mathbf{Q} \right) + \\ & \psi_{cs}^+ V_{\bar{q}_1 q_2}(\mathbf{Q}) \psi_{q_1 \bar{q}_1} \left(\mathbf{p}_{q'_1 \bar{q}'_1} + \frac{m_{q_1}}{m_{q_1} + m_{\bar{q}_1}} \mathbf{Q} \right) \times \\ & \psi_{q_2 \bar{q}_2} \left(\mathbf{p}_{q'_2 \bar{q}'_2} + \frac{m_{\bar{q}_2}}{m_{q_2} + m_{\bar{q}_2}} \mathbf{Q} \right) + \\ & \left. \psi_{cs}^+ V_{q_1 q_2}(\mathbf{Q}) \psi_{q_1 \bar{q}_1} \left(\mathbf{p}_{q'_1 \bar{q}'_1} - \frac{m_{\bar{q}_1}}{m_{q_1} + m_{\bar{q}_1}} \mathbf{Q} \right) \times \right. \\ & \psi_{q_2 \bar{q}_2} \left(\mathbf{p}_{q'_2 \bar{q}'_2} + \frac{m_{\bar{q}_2}}{m_{q_2} + m_{\bar{q}_2}} \mathbf{Q} \right) + \\ & \left. \psi_{cs}^+ V_{\bar{q}_1 \bar{q}_2}(\mathbf{Q}) \psi_{q_1 \bar{q}_1} \left(\mathbf{p}_{q'_1 \bar{q}'_1} + \frac{m_{q_1}}{m_{q_1} + m_{\bar{q}_1}} \mathbf{Q} \right) \times \right. \\ & \left. \psi_{q_2 \bar{q}_2} \left(\mathbf{p}_{q'_2 \bar{q}'_2} - \frac{m_{q_2}}{m_{q_2} + m_{\bar{q}_2}} \mathbf{Q} \right) \right], \quad (2) \end{aligned}$$

where \mathbf{Q} is the gluon momentum and m_i ($i = q_1, \bar{q}_1, q_2, \bar{q}_2$) is the mass of a constituent quark

or antiquark of mesons. For mesons $\psi_{ij}(\mathbf{p}_{ij})$, with \mathbf{p}_{ij} being the relative momentum of quark i and antiquark j the wave function of the quark-antiquark relative motion in momentum space satisfies $\int \frac{d^3 p_{ij}}{(2\pi)^3} \psi_{ij}^+(\mathbf{p}_{ij}) \psi_{ij}(\mathbf{p}_{ij}) = 1$. ψ_{cs} is the color-spin wave function of the final quarks and antiquarks. The potential $V_{ij}(\mathbf{Q})$ depends on temperature T

$$\begin{aligned} V_{ij}(\mathbf{Q}) = & \frac{\lambda_i}{2} \cdot \frac{\lambda_j}{2} \left[\frac{4\pi\alpha_s}{\mu^2(T) + \mathbf{Q}^2} + \frac{6\pi b(T)}{(\mu^2(T) + \mathbf{Q}^2)^2} - \right. \\ & \left. \frac{8\pi\alpha_s}{3m_i m_j} \mathbf{s}_i \cdot \mathbf{s}_j \exp\left(-\frac{\mathbf{Q}^2}{4d^2}\right) \right], \quad (3) \end{aligned}$$

where λ_i , \mathbf{s}_i and m_i are the Gell-Mann “ λ -matrices”, the spin and the mass of the constituent i , respectively; $d = 0.897 \text{ GeV}^{[5, 6]}$, $\alpha_s = \frac{12\pi}{25 \ln(10 + \mathbf{Q}^2/X^2)}$ with $X = 0.31 \text{ GeV}$, $b(T) = 0.35[1 - (T/T_c)^2]\theta(T_c - T) \text{ GeV}^2$ with $T_c = 0.175 \text{ GeV}$, and $\mu(T) = 0.28\theta(T_c - T) \text{ GeV}$. The constituent quark masses (CQM) are 0.334 GeV for both the u and d quarks and 0.575 GeV for the s quark in a fit to meson spectroscopy^[5]. The potential is the Fourier transform of the coordinate-space potential $\tilde{V}(\mathbf{r}_{ij})$ that takes a form Ref. [7] whose central interquark potential is obtained from the lattice gauge results of Karsch et al^[8]. The potential reflects the medium screening effect at finite temperature. It has been used to calculate temperature-dependent dissociation cross sections of $\pi + J/\psi$, $\pi + \chi_{c1}$ and $\pi + \chi_{c2}$ ^[9] in the quark-interchange mechanism^[10]. In hadronic physics heavy quark potential and light quark potential take the same form except for the running coupling constant and quark masses that rely on quark flavors. Therefore, the potential given by Karsch et al.^[8] applies here.

\mathcal{M}_{fi} is obtained from the matrix element

$$\begin{aligned} \langle q_1, \bar{q}_1, q_2, \bar{q}_2 | H_I | A, B \rangle = & \frac{(2\pi)^3 \delta(\mathbf{P}_i - \mathbf{P}_f) \mathcal{M}_{\text{fi}}}{V^3 \sqrt{2E_A 2E_B 2E_{q'_1} 2E_{\bar{q}'_1} 2E_{q'_2} 2E_{\bar{q}'_2}}}, \quad (4) \end{aligned}$$

where \mathbf{P}_i (\mathbf{P}_f) is the total three-dimensional momentum of the two initial mesons (final quarks and antiquarks); the wave functions of the initial mesons and of the final quarks and antiquarks are normalized to one in volume V , respectively. The interaction is

$$H_I = \tilde{V}(\mathbf{r}_{q_1 \bar{q}_2}) + \tilde{V}(\mathbf{r}_{\bar{q}_1 q_2}) + \tilde{V}(\mathbf{r}_{q_1 q_2}) + \tilde{V}(\mathbf{r}_{\bar{q}_1 \bar{q}_2}). \quad (5)$$

Denote the orbital angular momentum and the spin of meson A (B) by L_A (L_B) and S_A (S_B), respec-

tively. The unpolarized cross section

$$\sigma_{AB \rightarrow \text{free}}^{\text{unpol}}(\sqrt{s}) = \frac{1}{(2S_A+1)(2S_B+1)(2L_B+1)} \times \sum_{L_{Bz} S S_{q'_1+\bar{q}'_1} S_{q'_2+\bar{q}'_2}} (2S+1) \times \sigma(L_{Bz}, S, m_S, S_{q'_1+\bar{q}'_1}, S_{q'_2+\bar{q}'_2}, \sqrt{s}), \quad (6)$$

establishes for the three cases: (1) $L_A = L_B = 0$, (2) $L_A = 0$, $L_B \neq 0$, $S_A = 0$, (3) $L_A = 0$, $L_B = 1$, $S_A = 1$, $S_B = 1$. L_{Bz} is the magnetic quantum number of meson B, S is the total spin of the two mesons and its component is m_S . $S_{q'_1+\bar{q}'_1}$ ($S_{q'_2+\bar{q}'_2}$) is the total spin of the final constituents q_1 and \bar{q}_1 (q_2 and \bar{q}_2). σ is independent of m_S and is calculated at any value subject to the condition $-S \leq m_S \leq S$.

The momentum-space wave functions used in the transition amplitude are Fourier transform of the temperature-dependent solutions of the Schrödinger equation with the temperature-dependent potential $\tilde{V}(\mathbf{r}_{ij})^{[7]}$. Cross sections depend on temperature as well as the center-of-mass energy of the two initial mesons. While temperature increases, the confinement potential becomes weak and the bound states becomes loose. At higher temperature stronger screening leads to larger cross sections for meson-meson reactions. Due to the number of pages limited by the Editorial Board, only the cross sections for $\pi + \pi \rightarrow q_1 + \bar{q}_1 + q_2 + \bar{q}_2$ is shown in Fig. 2. At zero temperature the cross sections are very small and completely negligible. Hence no free quarks and antiquarks are observed at zero temperature or in vacuum. This has already been verified in Refs. [11, 12] in the case of $\pi + J/\psi \rightarrow q_1 + \bar{q}_1 + c + \bar{c}$ with different potentials. Cross sections determine whether or not the asymptotic state can be produced in reactions.

To uniquely show the role of $A(q_1\bar{q}_1) + B(q_2\bar{q}_2) \rightarrow q_1 + \bar{q}_1 + q_2 + \bar{q}_2$, we do not consider any expansion of hadronic matter. The master rate equations for free quarks, π , ρ , K and K^* in static hadronic matter are

$$\frac{dn_q}{dt} = \sum_{i=\pi,\rho,K,K^*} \sum_{j=\pi,\rho,K,K^*} \langle v_{\text{rel}} \sigma_{ij \rightarrow \text{free}}^{\text{unpol}} \rangle n_i n_j, \quad (7)$$

$$\frac{dn_\pi}{dt} = - \sum_{j=\pi,\rho,K,K^*} \langle v_{\text{rel}} \sigma_{\pi j \rightarrow \text{free}}^{\text{unpol}} \rangle n_\pi n_j, \quad (8)$$

$$\frac{dn_\rho}{dt} = - \sum_{j=\pi,\rho,K,K^*} \langle v_{\text{rel}} \sigma_{\rho j \rightarrow \text{free}}^{\text{unpol}} \rangle n_\rho n_j, \quad (9)$$

$$\frac{dn_K}{dt} = - \sum_{j=\pi,\rho,K,K^*} \langle v_{\text{rel}} \sigma_{K j \rightarrow \text{free}}^{\text{unpol}} \rangle n_K n_j, \quad (10)$$

$$\frac{dn_{K^*}}{dt} = - \sum_{j=\pi,\rho,K,K^*} \langle v_{\text{rel}} \sigma_{K^* j \rightarrow \text{free}}^{\text{unpol}} \rangle n_{K^*} n_j, \quad (11)$$

where n_q , n_π , n_ρ , n_K and n_{K^*} are the number densities of free quarks, π , ρ , K and K^* , respectively; v_{rel} in the thermal averages denoted by the symbols, $\langle \dots \rangle$ is the relative velocity of two colliding hadrons. The number density of free antiquarks equals the one of free quarks.

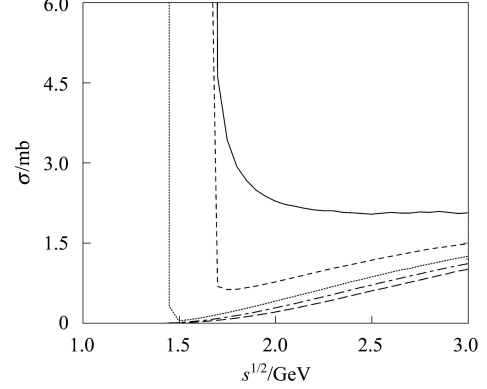


Fig. 2. Cross sections for π — π scattering into free quarks and antiquarks with the constituent quark masses at $T = 0.14$ GeV (long dashed), 0.15 GeV (dot-dashed), 0.16 GeV (dotted), 0.174 GeV (dashed). The solid curve denotes the cross section in the chiral limit at $T = 0.174$ GeV.

3 Numerical results and discussions

We assume that at $t = 0$ fm/c matter below T_c is pure hadronic matter in thermal and chemical equilibrium. The initial number densities of free quarks and antiquarks equal zero, respectively, and the ones for π , ρ , K and K^* are given by $n_j = \int \frac{d^3 p_j}{(2\pi)^3} \frac{g_j}{\exp(\sqrt{\mathbf{p}_j^2 + m_j^2}/T) - 1}$ with the degeneracy factor g_j , the meson mass m_j and $j = \pi, \rho, K, K^*$. The master rate equations give solutions as functions of time at different temperatures as plotted in Figs. 3—5. When more and more hadrons due to the collisions convert into free quarks and antiquarks, the number densities increase for free quarks and decrease for the mesons. The number densities vary faster at higher temperature due to larger cross sections. The loss of chemical equilibrium of hadronic matter is obvious. If we include the recombination of quarks and antiquarks to form mesons M via $q + \bar{q} \rightarrow M + g$, the cross section for the reaction of radiating a gluon is calculated with Eq. (6.1) of Ref. [13]. The results of this recombination are that the number density of free quarks or antiquarks in the chiral limit at $T = 0.174$ GeV is reduced by about 2% at $t = 1$ fm/c, the ones with the constituent quark

masses at $T = 0.174, 0.16, 0.15$ and 0.14 GeV are reduced by about 0.9%, 0.4%, 0.2% and 0.06%, respectively. Since the number densities of free quarks and antiquarks are generally not high in the small time interval of $1 \text{ fm}/c$, the recombination of quarks and antiquarks to form mesons can be neglected. But the variation of number densities during this small period is enough for us to draw conclusions.

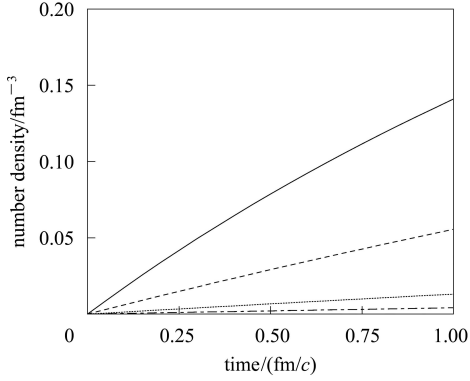


Fig. 3. Number densities of free quarks or antiquarks with the constituent quark masses at $T = 0.15$ GeV (dot-dashed), 0.16 GeV (dotted), 0.174 GeV (dashed). The solid curve denotes the number density in the chiral limit at $T = 0.174$ GeV.

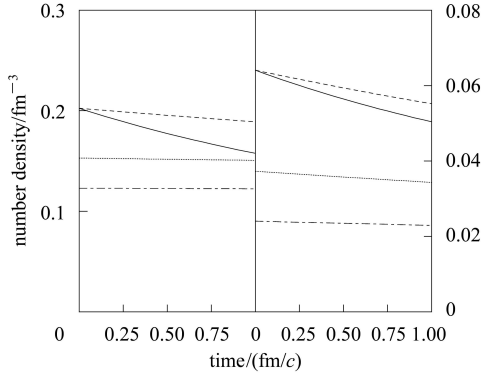


Fig. 4. The same as Fig. 3 except for pions in the left panel and rhos in the right panel.

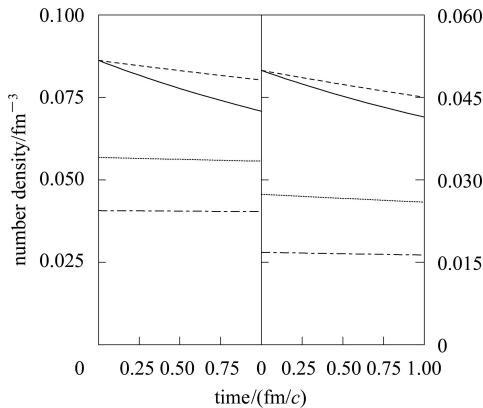


Fig. 5. The same as Fig. 3 except for kaons in the left panel and vector kaons in the right panel.

We present two solutions for $T = 0.174$ GeV near the critical temperature. The solution shown by the dashed curves is obtained for the final quarks and antiquarks taking the constituent quark masses. The other solution shown by the solid curves corresponds to the chiral limit (CL) of final quarks and antiquarks. A comparison of the five dashed curves shows that the number density of free quarks can exceed the ones of ρ and K^* in the small time interval of $1 \text{ fm}/c$ while in the chiral limit n_q can become larger than n_ρ , n_K and n_{K^*} .

Table 1. Ratios of number densities at $t = 1 \text{ fm}/c$.

T/GeV	n_q/n_π	n_q/n_ρ	n_q/n_K	n_q/n_{K^*}	$n_q/(n_\pi + n_\rho + n_K + n_{K^*})$
0.174 (CL)	0.89	2.80	1.99	3.40	0.44
0.174 (CQM)	0.29	1.01	0.69	1.23	0.15
0.16	0.09	0.38	0.23	0.50	0.05
0.15	0.03	0.18	0.10	0.25	0.02
0.14	0.01	0.08	0.04	0.12	0.01

The ratios of the number densities of free quarks to the mesons are listed in Table 1. The number density of hadronic matter is approximately equal to $n_\pi + n_\rho + n_K + n_{K^*}$. The first and second rows are obtained in the chiral limit and in the use of the constituent quark masses, respectively. An entry in the first row is about three times the entry in the same column in the second row. This means that hadrons convert quickly into free quarks and antiquarks while the chiral symmetry is restored. At $T = 0.16$ GeV a certain amount of free quarks exist in hadronic matter. At $T < 0.14$ GeV, free quarks can be neglected because the ratio $n_q/(n_\pi + n_\rho + n_K + n_{K^*})$ is very small. If we define the critical temperature as the temperature at which free quarks begin to appear, T_c should be 0.14 GeV and get smaller compared to 0.175 GeV. The present definition of the critical temperature is that at the temperature all hadrons become free quarks and antiquarks. Hence, the effect of the meson-meson collisions on the critical temperature depends on the definition of the critical temperature. At least the meson-meson collisions do not increase the critical temperature.

The temperature-dependent potential in Eq. (3) was used by Wong^[7] to calculate charmonium spectroscopy. Since the potential has already contained T_c in the known function $b(T)$, it is meaningless to determine the value of the critical temperature from any results of the potential. However, one can seek to get the critical temperature from the original data of the potential offered by the lattice gauge calculations^[8]. Karsch et al. adopted T_c as the middle of the temperature region of the most rapid fall of the data^[8].

As the first step when we study the role of $A(q_1\bar{q}_1) + B(q_2\bar{q}_2) \rightarrow q_1 + \bar{q}_1 + q_2 + \bar{q}_2$, we haven't considered the quark-antiquark annihilation processes. If the contribution of the annihilation processes was included, more quarks and antiquarks would be produced as the following estimate shows. Like the simple estimate of hadron-hadron cross sections in Ref. [14], we estimate the ratio of the cross section σ_{Aij} for the meson-meson reaction caused by the quark-antiquark annihilation processes to the cross section σ_{OGEij} for the meson-meson reaction arising from one gluon exchange between two constituents individually belonging to the two mesons i and j . For low-energy pp and p \bar{p} reactions, their cross sections are comparable $\sigma_{pp} \sim \sigma_{p\bar{p}}$ ^[15]. The low-energy pp cross section originates from the contribution of one gluon exchange between two constituents and the low-energy p \bar{p} cross section comes from the contribution of quark-antiquark annihilation processes. In the treatment, the hadron-hadron cross section amounts to the sum of constituent-constituent cross sections^[14], including the isospin degeneracy factor g_i of a meson i , and we get $g_{1\pi}g_{1\pi}\sigma_{OGE\pi\pi} \sim 9 \times \frac{4}{9}\sigma_{pp}$ and $g_{1\pi}g_{1\pi}\sigma_{A\pi\pi} \sim \frac{9}{9}\sigma_{p\bar{p}}$ which lead to the ratio $\sigma_{A\pi\pi}/\sigma_{OGE\pi\pi} \sim 1/4$. Neglecting the difference of the strange quark mass and the up quark mass, for other reactions we have

$$\begin{aligned} g_{1\pi}g_{1K}\sigma_{OGE\pi K} &\sim 12 \times \frac{4}{9}\sigma_{pp}, & g_{1\pi}g_{1K}\sigma_{A\pi K} &\sim \frac{6}{9}\sigma_{p\bar{p}}, \\ \sigma_{A\pi K}/\sigma_{OGE\pi K} &\sim 1/8, & g_{1K}g_{1K}\sigma_{OGEK K} &\sim 16 \times \frac{4}{9}\sigma_{pp}, \\ g_{1K}g_{1K}\sigma_{AKK} &\sim \frac{12}{9}\sigma_{p\bar{p}}, & \sigma_{AKK}/\sigma_{OGEK K} &\sim 1/5, \\ \sigma_{A\rho\rho}/\sigma_{OGE\rho\rho} &\sim 1/4, & \sigma_{A\pi\rho}/\sigma_{OGE\pi\rho} &\sim 1/4, \\ \sigma_{A\pi K^*}/\sigma_{OGE\pi K^*} &\sim 1/8, & \sigma_{A\rho K}/\sigma_{OGE\rho K} &\sim 1/8, \\ \sigma_{A\rho K^*}/\sigma_{OGE\rho K^*} &\sim 1/8, & \sigma_{AK^*K^*}/\sigma_{OGEK^*K^*} &\sim 1/5, \\ \sigma_{AKK^*}/\sigma_{OGEK K^*} &\sim 1/5. \end{aligned}$$

References

- 1 Karsch F. Lecture Notes in Physics, **583**, Springer, Berlin, 2002. 209
- 2 Adler S S et al. PHENIX Collaboration. Phys. Rev. C, 2004, **69**: 034909
- 3 Adams J et al. STAR Collaboration. Phys. Rev. Lett., 2004, **92**: 092301
- 4 Bearden I G et al. (BRAHMS Collaboration). Phys. Rev. Lett., 2003, **90**: 102301; Bearden I G et al. (BRAHMS Collaboration). Phys. Rev. Lett., 2005, **94**: 162301
- 5 Wong C Y, Swanson E S, Barnes T. Phys. Rev. C, 2001, **65**: 014903
- 6 Barnes T, Swanson E S, Wong C Y, XU X M. Phys. Rev. C, 2003, **68**: 014903

The values of the above ratios may extend to temperature-dependent cross sections for $A(q_1\bar{q}_1) + B(q_2\bar{q}_2) \rightarrow q_1 + \bar{q}_1 + q_2 + \bar{q}_2$ since the realistic calculations of both σ_{OGEij} and σ_{Aij} involve the same temperature-dependent wave function of the quark-antiquark relative motion. The cross section σ_{OGEAB} for $A(q_1\bar{q}_1) + B(q_2\bar{q}_2) \rightarrow q_1 + \bar{q}_1 + q_2 + \bar{q}_2$ has been employed in the master rate equations. Because dn_q/dt is proportional to the meson-meson cross sections, the quark-antiquark annihilation processes added to the master rate equations are expected to increase the number density of free quarks or antiquarks over 12%.

Shown in Figs. 4 and 5, the number densities of pions, rhos, kaons and vector kaons are low. Hence the probabilities for three-meson collisions into three quarks and three antiquarks in comparison with the two-meson collisions are suppressed not only by the small quark-gluon coupling constant but also by the low number densities of the four types of mesons. Only when the number densities are very high to compensate for the small quark-gluon coupling constant, will the three-meson collisions become important, but this is not realistic in hadronic matter. In addition, it is very difficult to calculate transition matrix elements for the three-meson collisions.

4 Conclusions

We have found that the reaction $A(q_1\bar{q}_1) + B(q_2\bar{q}_2) \rightarrow q_1 + \bar{q}_1 + q_2 + \bar{q}_2$ becomes important in hadronic matter at high temperature because of the medium screening effect. Due to the reactions of π , ρ , K and K^* , matter below T_c consists of free quarks, free antiquarks and hadrons. The reaction is a new dynamical process for the deconfinement transition of hadronic matter.

We thank Professor C.-Y. Wong for his interesting remarks.

- 7 Wong C Y. Phys. Rev. C, 2002, **65**: 034902
- 8 Karsch F, Laermann E, Peikert A. Nucl. Phys. B, 2001, **605**: 579
- 9 XU X M, Wong C Y, Barnes T. Phys. Rev. C, 2003, **67**: 014907
- 10 Barnes T, Swanson E S. Phys. Rev. D, 1992, **46**: 131; Swanson E S. Ann. Phys. (N.Y.), 1992, **220**: 73
- 11 Martins K, Blaschke D, Quack E. Phys. Rev. C, 1995, **51**: 2723
- 12 XU X M. Nucl. Phys. A, 2002, **697**: 825
- 13 Wong C Y. J. Phys. G, 2002, **28**: 2349
- 14 Lee T D. Particle Physics and Introduction to Field Theory. New York: Harwood Academic Publishers, 1983
- 15 Particle Data Group. J. Phys. G, 2006, **33**: 1